On Variations in the Peak Luminosity of Type Ia Supernovae

Frank X. Timmes (T-6), Edward F. Brown (Michigan State University), and J. W. Truran (University of Chicago)

We explore the idea that the observed variations in the peak luminosities of Type Ia supernovae originate in part from a scatter in metallicity of the main-sequence stars that become white dwarfs. Previous, numerical, studies have not self-consistently explored metallicities greater than solar. One-dimensional Chandrasekhar mass models of Type Ia supernovae produce most of their radioactive nickel in a thermonuclear burn to nuclear statistical equilibrium between where the electron to nucleon ratio is constant. We show analytically that, under these conditions, charge and mass conservation constrain the mass of nickel produced to depend linearly on the original metallicity of the white dwarf progenitor. This curious result is independent of any complicated hydrodynamics or flame propagation microphysics, and 3-dimensional (3D) explosion models confirm this linear dependence. The observed factor of three scatter in the metallicity of solar neighborhood stars is enough to induce a 25% variation in the mass of nickel ejected by Type Ia supernova, which is enough to vary the peak luminosity of Type Ia events by about 0.2 magnitudes in the visual band. We argue that this intrinsic scatter in the peak luminosity is present in spirals and elliptical galaxies out to the limiting redshifts of current observations.

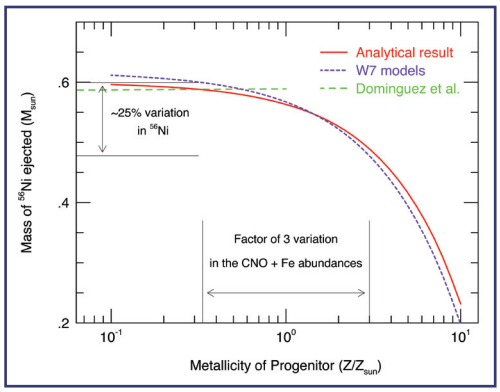

Figure 1—
Mass of ^{56}Ni ejected by Type Ia Supernovae as a function of the initial metallically Z. Shown is the linear relation (red curve; the curvature is from the logarithmic abscissa), and two popular 1-dimensional models (purple and green curves). As indicated by the arrows, a scatter in the abundances with which a low mass star is born leads to a variation of about 25% of ^{56}Ni ejected if the metals are uniformly distributed within the remnant white dwarf. A factor of seven scatter about the mean in the initial metallicity corresponds to a factor of 2 variation in M(Ni).

Nearly all 1D Chandrasekhar mass models of Type Ia supernova produce most of their ^{56}Ni in a burn to nuclear statistical equilibrium between the mass shells 0.2 $M_\odot$ and 0.8 $M_\odot$. In this region, unlike in the innermost 0.2 $M_\odot$ weak interactions operate on timescales longer than the time for the thermonuclear burning front to disrupt the white dwarf. Following this rapid burn to nuclear statistical equilibrium, most of the mass is in the iron-peak nuclei ^{56}Ni, ^{58}Ni, and ^{54}Fe. First consider the case when ^{56}Ni and ^{58}Ni are the only two competing species. Mass and charge conservation,

$$\sum_{i=1}^{n} X_i = 1, \sum_{i=1}^{n} \frac{Z_i}{A_i} X_i = Y_e$$

imply that the mass fraction of ^{56}Ni depends linearly on Y_e,

$$X(^{56}Ni) = 58\mathrm{Y}_e - 28,$$

where isotope i has Z_i protons, A_i nucleons (protons + neutrons), and a mass fraction X_i. The aggregate ensemble has a proton to nucleon ratio of Y_e.

In the white dwarf progenitors of Type Ia supernovae, the surplus neutrons come from ^{22}Ne formed from the original CNO of the progenitor main-sequence star, and from the original ^{56}Fe. Using this to compute only unknown, Y_e, we find

$$X\left(^{56}Ni\right) = \left(1 - 0.057 \frac{Z}{Z_\odot}\right).$$

The total mass of ^{56}Ni ejected is then

$$X\left(^{56}Ni\right) \approx 0.6\left(1 - 0.057 \frac{Z}{Z_\odot}\right) M_\odot .$$

This linear relation is shown by the red line in Fig. 1 along with the results of our post-processing calculation (purple dashed line) of a standard one-dimensional model of Type Ia supernovae (courtesy F. Brachwitz and F. Thielemann). Our analytical result [1] and postprocessing result are in good agreement with those of Refs. [2, 3] and (green dotted line) where the calculations overlap in metallicity. Our findings disagree, however, with those of [4], who found only a 4% variation in M(^{56}Ni) over an even larger range of Z (0.1 to 10 times solar).

The Max-Planck group in Germany [5], and the ASC/Alliance Center at the University of Chicago [6] have recently explored the dependence of the M(^{56}Ni) abundance on the initial metallicity, as reflected in X(^{22}Ne), with 2D and 3D calculations. The temperature field of our 2D calculations is shown in the impressionistic Seurat-like pointillism of Fig. 2. Both of these groups substantially reproduce the analytic result (Fig. 3).

The general trend among field stars is that the metallicity rises rapidly and then increases gradually over the last 10 Gyr corresponding to redshifts z ¡ 1. The scatter in the abundances is roughly from 1/3 to 3 times solar at all ages, and this scatter in the material from which stars are born is sufficient to induce a 25% variation (0.13 $M_{\odot}$) in the mass of M(^{56}Ni) ejected. The minimum peak brightness variations caused by this variation in ^{56}Ni mass are $\Delta M_v \sim 0.2$.

For the nearby Type Ia supernovae with Cepheid determined distances, the overall dispersion in the peak magnitude is rather small, about 0.5 magnitude in the B and V bands [7, 8]. When the sample is enlarged to include more distant supernovae, there are several subluminous events that broaden the variation to about 1 magnitude in B [9, 10], but the bulk of the Type Ia sample lies within 0.5 magnitude in B. While the magnitude of analytic effect that we have identified cannot account for all of the observed variation in peak luminosity of local Type Ia supernovae, it is probably the largest contributor [11].

[1] Timmes et al., *Ap. J. L.*, **590**, L83 (2003).
[2] Iwamoto et al., *Ap. J. S.*, **125**, 439 (1999).
[3] Domínguez, et al., "Constraints on the Progenitors of Type Ia Supernovae and Implications for the Cosmological Equation of State," *Astrophys. J.* **557**, 279–291 (2001).
[4] Höflich et al., *Astrophys. J. S.* **495**, 617 (1998).
[5] Travaglio et al., *A&A* **425**, 1029 (2004).
[6] Brown et al., to be published in *Nucl. Phys. A*, 2005.

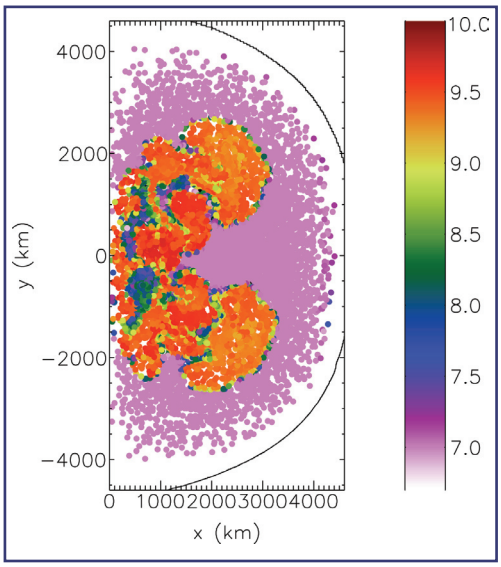

Figure 2—
Nickel mass from a two-dimensional calculation performed at the ASC Alliance Center the University of Chicago [6]. The strong 45˚ symmetry in the Seraut-like image is due to artificial symmetries present in the initial conditions.

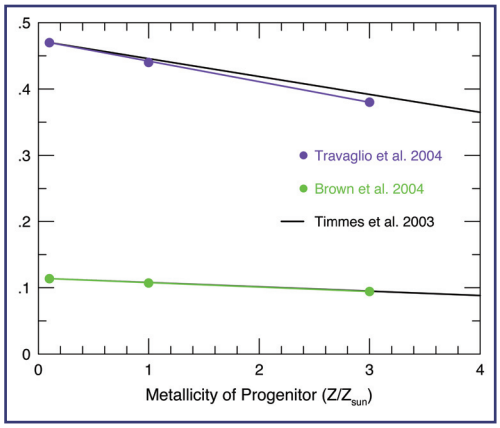

Figure 3—
Nickel mass from three-dimensional (purple curve) and two-dimensional (green curve) simulations. The linear relationship of the analytical formula (black curve) is largely reproduced. The difference between the 3D and 2D results has less to do with the dimensionality of the calculation and more to do with how the burning front is modeled.

[7] Saha et al., *Ap. J.*, **522**, 802 (1999).
[8] Gibson et al., *Ap. J.* **529**, 723 (2000).
[9] Hamuy et al., *Astron. J.* **112**, 2438 (2004).
[10] Riess et al., *A.J.* **106**, 1009 (2004).
[11] F.K. Roepke and W. Hillebrandt, *A&A* **420**, L1 (2004).

For more information, contact Francis Timmes (timmes@lanl.gov).

Acknowledgements
We would like to acknowledge NNSA's Advanced Simulation and Computing (ASC), Verification and Validation Program and Alliance Center Program for financial support.